

## THE DISK FRACTIONS OF BROWN DWARFS IN IC 348 AND CHAMAELEON I<sup>1</sup>

K. L. LUHMAN<sup>2,3</sup>, C. J. LADA<sup>2</sup>, L. HARTMANN<sup>2</sup>, A. A. MUENCH<sup>2</sup>, S. T. MEGEATH<sup>2</sup>, L. E. ALLEN<sup>2</sup>, P. C. MYERS<sup>2</sup>, J. MUZEROLLE<sup>4</sup>, E. YOUNG<sup>4</sup>, AND G. G. FAZIO<sup>2</sup>

*Draft version November 15, 2018*

### ABSTRACT

Using the Infrared Array Camera (IRAC) aboard the *Spitzer Space Telescope*, we have obtained mid-infrared photometry for 25 and 18 low-mass members of the IC 348 and Chamaeleon I star-forming clusters, respectively ( $>M6$ ,  $M \lesssim 0.08 M_{\odot}$ ). We find that  $42 \pm 13\%$  and  $50 \pm 17\%$  of the two samples exhibit excess emission indicative of circumstellar disks. In comparison, the disk fractions for stellar members of these clusters are  $33 \pm 4\%$  and  $45 \pm 7\%$  ( $M0-M6$ ,  $0.7 M_{\odot} \gtrsim M \gtrsim 0.1 M_{\odot}$ ). The similarity of the disk fractions of stars and brown dwarfs is consistent with a common formation mechanism and indicates that the raw materials for planet formation are available around brown dwarfs as often as around stars.

*Subject headings:* accretion disks – planetary systems: protoplanetary disks – stars: formation — stars: low-mass, brown dwarfs — stars: pre-main sequence

### 1. INTRODUCTION

Because planets are born in dusty circumstellar disks, the likelihood of planet formation around brown dwarfs relative to that among stars can be constrained in part by comparing the prevalence of disks between these two mass regimes. Given the central role of disks in the star formation process, a comparison of disk fractions of brown dwarfs and stars also would help determine if they share common formation mechanisms. Extensive work has been done in measuring disk fractions for stars (e.g., Kenyon & Hartmann 1995; Haisch, Lada, & Lada 2001), which typically consists of infrared (IR) photometry of a significant fraction of a young stellar population and identification of the objects with excess emission indicative of cool, dusty disks. In recent years, this method of detecting disks has been applied to objects near and below the hydrogen burning mass limit using photometry at 2-3  $\mu\text{m}$  (Luhman 1999, 2004c; Lada et al. 2000, 2004; Muench et al. 2001; Liu et al. 2003; Jayawardhana et al. 2003), 4-15  $\mu\text{m}$  (Persi et al. 2000; Comerón et al. 2000; Natta & Testi 2001; Pascucci et al. 2003; Apai et al. 2004; Sterzik et al. 2004; Mohanty et al. 2004), and millimeter wavelengths (Klein et al. 2003). However, detections of disks with the data at 2-3  $\mu\text{m}$  have been difficult because the emitting regions for these wavelengths become very small for disks around low-mass bodies. Meanwhile, disk excesses are larger at longer wavelengths, but have been measured for only a small number of the brighter, more massive objects because of technological limitations. In comparison, because the *Spitzer Space*

*Telescope* is far more sensitive beyond 3  $\mu\text{m}$  than any other existing facility and can survey large areas of sky, it can reliably and efficiently detect disks for brown dwarfs at very low masses (Luhman et al. 2005a) and for large numbers of brown dwarfs in young clusters.

To capitalize on the unique capabilities of *Spitzer* for measuring disk fractions, we have used the Infrared Array Camera (IRAC; Fazio et al. 2004) to obtain mid-IR photometry for spectroscopically confirmed stellar and substellar members of the star-forming clusters IC 348 (e.g., Herbig 1998; Luhman et al. 2003) and Chamaeleon I (e.g., Comerón et al. 2004; Luhman 2004a). In this Letter, we describe these observations, identify the cluster members that exhibit mid-IR excesses indicative of dusty inner disks, compare the disk fractions of brown dwarfs and stars, and discuss the resulting implications for the formation mechanism of brown dwarfs and planet formation around brown dwarfs.

### 2. OBSERVATIONS

As a part of the Guaranteed Time Observations of the IRAC instrument team, we obtained images of IC 348 and Chamaeleon I at 3.6, 4.5, 5.8, and 8.0  $\mu\text{m}$  with IRAC on the *Spitzer Space Telescope*. We performed seven sets of observations: three large shallow maps of IC 348 and the northern and southern clusters in Chamaeleon I, one small deep map of IC 348, two small deep maps of the southern cluster in Chamaeleon I, and a single position toward the low-mass binary 2MASS J11011926-7732383 on the southwestern edge of Chamaeleon I (Luhman 2004b). The characteristics of these maps are summarized in Table 1. Further details of the observations and data reduction for IC 348 and the northern cluster of Chamaeleon I are provided by Lada et al. (in preparation) and Luhman et al. (2005a), respectively. Similar methods were used for the remaining maps in Table 1. For all data, we have adopted zero point magnitudes ( $ZP$ ) of 19.670, 18.921, 16.855, and 17.394 in the 3.6, 4.5, 5.8 and 8  $\mu\text{m}$  bands, where  $M = -2.5 \log(DN/sec) + ZP$  (Reach et al. 2005). These values of  $ZP$  differ slightly from those used for OTS 44 by Luhman et al. (2005a) and for Taurus by Hartmann et al. (2005). In Tables 2

<sup>1</sup> This work is based on observations made with the *Spitzer Space Telescope*, which is operated by the Jet Propulsion Laboratory, California Institute of Technology under NASA contract 1407. Support for this work was provided by NASA through contract 1256790 issued by JPL/Caltech. Support for the IRAC instrument was provided by NASA through contract 960541 issued by JPL.

<sup>2</sup> Harvard-Smithsonian Center for Astrophysics, 60 Garden St., Cambridge, MA 02138; kluhman, clada, lhartmann, gmuench, tmegeath, leallen, pmyers, gfazio@cfa.harvard.edu.

<sup>3</sup> Current address: Department of Astronomy and Astrophysics, The Pennsylvania State University, University Park, PA 16802.

<sup>4</sup> Steward Observatory, The University of Arizona, Tucson, AZ 85721; jamesm, eyoung@as.arizona.edu.

and 3, we list IRAC photometry for all known members of IC 348 and Chamaeleon I that are likely to be brown dwarfs ( $>M6$ )<sup>5</sup> and that are within our images. Measurements for the earlier, stellar members of these clusters will be tabulated in forthcoming studies. An absent measurement in Table 2 indicates that the object was below the detection limit in that filter. Because of the weaker background emission in Chamaeleon I, the detection limits are much better in that cluster, and all objects in Table 3 have extrapolated photospheric fluxes above the detection limits for all four bands. Thus, an absent measurement in Table 3 indicates contamination by cosmic rays or a position beyond the map’s field of view.

### 3. ANALYSIS

To measure disk fractions in IC 348 and Chamaeleon I, we first define the samples of stars and brown dwarfs that will be used. We consider all known members of IC 348 (Luhman et al. 2003, 2005b, references therein) and Chamaeleon I (Luhman 2004a; Luhman et al. 2004; Comerón et al. 2004, references therein) that have measured spectral types of M0 or later ( $M \lesssim 0.7 M_{\odot}$ ) and detections in our IRAC images. This spectral type range encompasses most of the known members of each cluster ( $> 80\%$ ). Because many of the known members of Chamaeleon I were originally discovered through the presence of signatures directly or indirectly related to disks (IR excess, H $\alpha$  emission), membership samples from earlier studies of the cluster are potentially biased toward objects with disks, which would preclude a meaningful disk fraction measurement. Therefore, to ensure that we have an unbiased sample of members of Chamaeleon I, we include in our analysis the additional members discovered during a new magnitude-limited survey of the cluster (Luhman, in preparation)<sup>6</sup>. Finally, for the purposes of this work, we treat as members of IC 348 the two candidates from Luhman et al. (2005b), sources 1050 and 2103. The resulting samples for IC 348 and Chamaeleon I contain 246 and 109 objects, respectively.

To identify objects with disks in the samples we have defined for IC 348 and Chamaeleon I, we use an IRAC color-color diagram consisting of [3.6]-[4.5] versus [4.5]-[5.8]. The dependence of these colors on extinction and spectral type is very small for the range of extinctions and types in question. Most of the objects in our samples exhibit  $A_V < 4$ , which corresponds to  $E([3.6] - [4.5]) < 0.04$  and  $E([4.5] - [5.8]) < 0.02$ . The effect of spectral type on these colors was determined by computing the average colors as a function of spectral type of objects within the (diskless) clump of members

near the origin in the color-color diagram of each cluster in Figure 1. This analysis indicates that the intrinsic [3.6]-[4.5] can be fit by two linear relations between [3.6] - [4.5] = 0.01, 0.105, and 0.13 at M0, M4, and M8, respectively, while the [4.5]-[5.8] colors show no dependence on spectral type and have an average value of 0.06. In comparison, colors using bands shorter than [3.6] are more sensitive to extinction and spectral type, and thus are less attractive choices for this analysis. Meanwhile, measurements at 8.0  $\mu\text{m}$  are available for fewer objects than the three shorter IRAC bands, primarily because of the bright reflection nebulosity in IC 348.

In Figure 1, we plot [3.6]-[4.5] versus [4.5]-[5.8] for the samples in IC 348 and Chamaeleon I. One of the two colors is unavailable for 24 and 18 objects (12 and 4 at  $>M6$ ) in these samples, respectively, and thus are not shown. In addition to these samples of cluster members, we include in Figure 1 all objects in the IRAC images that have been classified as field stars in previous studies (e.g., Luhman et al. 2003; Luhman 2004a), which correspond to 81 and 99 stars toward IC 348 and Chamaeleon I, respectively. We use these field stars as diskless control samples to gauge the scatter in colors due to photometric errors. The scatter in the field stars toward Chamaeleon I is actually larger than that of the clump of members near the origin, probably because the field stars are more heavily weighted toward fainter levels. According to the distributions of [3.6]-[4.5] and [4.5]-[5.8] for the field stars in Figure 1, excesses greater than 0.1 in both colors represent a significant detection of disk emission. These color excesses also coincide with a natural break in the distribution of colors for members of Taurus (Hartmann et al. 2005) and Chamaeleon I (Figure 1). A break of this kind is present but less well-defined in IC 348, probably because of the larger photometric errors caused by the brighter background emission. Therefore, we used these color excess criteria to identify objects with disks among the members of Chamaeleon I and IC 348 in Figure 1. To compute the color excesses of the cluster members, we adopted the intrinsic colors as a function of spectral type derived earlier in this section. This analysis produces disk fractions of 69/209 (M0-M6) and 8/13 ( $>M6$ ) in IC 348 and 35/77 (M0-M6) and 7/14 ( $>M6$ ) in Chamaeleon I. Among the members that are not plotted in Figure 1 (i.e., lack photometry at 3.6, 4.5, or 5.8  $\mu\text{m}$ ), 4/11 and 2/11 in IC 348 and 6/14 and 2/4 in Chamaeleon I exhibit significant excesses in the other available colors (e.g.,  $K$ -[4.5], [4.5]-[8.0]), while sources 621 and 761 in IC 348 have uncertain IRAC measurements and therefore are excluded. After accounting for these additional objects, we arrive at disk fractions of 73/220=33 $\pm$ 4% (M0-M6) and 10/24=42 $\pm$ 13% ( $>M6$ ) in IC 348 and 41/91=45 $\pm$ 7% (M0-M6) and 9/18=50 $\pm$ 17% ( $>M6$ ) in Chamaeleon I.

Disks with inner holes extending out to  $\sim 1$  AU can be undetected in the colors we have used, but they can have strong excess emission at longer wavelengths (Calvet et al. 2002; Forrest et al. 2004). For instance, source 316 in IC 348 exhibits excess emission at 8  $\mu\text{m}$  but not in the shorter bands. Thus, our measurements apply only to inner disks that are capable of producing significant excesses shortward of 6  $\mu\text{m}$  and represent lower limits to the total disk fractions.

<sup>5</sup> The hydrogen burning mass limit at ages of 0.5-3 Myr corresponds to a spectral type of  $\sim M6.25$  according to the models of Baraffe et al. (1998) and Chabrier et al. (2000) and the temperature scale of Luhman et al. (2003).

<sup>6</sup> In this survey, candidate low-mass stars and brown dwarfs across all of Chamaeleon I were identified through color-magnitude diagrams constructed from  $JHK_s$  photometry from the Two-Micron All-Sky Survey (2MASS) and  $i$  photometry from the Deep Near-Infrared Survey of the Southern Sky (DENIS). Additional candidates at fainter levels were identified with deeper optical and near-IR images of smaller fields toward the northern and southern clusters. These candidates were then classified as field stars or members through followup spectroscopy. The resulting completeness was similar to that achieved on other surveys using the same methods (e.g., Luhman et al. 2003; Luhman & Steeghs 2004).

## 4. DISCUSSION

We examine the implications of our brown dwarf disk fractions by first considering previous measurements of this kind in IC 348 and Chamaeleon I. Using *JHKL'* photometry, Jayawardhana et al. (2003) searched for evidence of disks among 53 objects in IC 348, Taurus,  $\sigma$  Ori, Chamaeleon I, the TW Hya association, Upper Scorpius, and Ophiuchus, 27 of which are later than M6<sup>7</sup>. When sources at all spectral types were combined (i.e., both low-mass stars and brown dwarfs), the resulting disk fractions for individual clusters exhibited large statistical errors of  $\sim 25\%$ . Better statistics were possible for a sample combining Chamaeleon I, IC 348, Taurus, and U Sco, for which Jayawardhana et al. (2003) found a disk fraction of 40-60%. For the objects with types of  $\leq M6$ , we find that the disk/no disk classifications of Jayawardhana et al. (2003) agree well with those based on our IRAC data. However, we find no excess emission in the IRAC colors for 2/3 objects later than M6 in IC 348 and Chamaeleon I (Cha H $\alpha$  7 and 12) that were reported to have disks by Jayawardhana et al. (2003).

An *L'*-band survey similar to that of Jayawardhana et al. (2003) was performed by Liu et al. (2003). They considered a sample of 7 and 32 late-type members of Taurus and IC 348, respectively, 12 of which have optical spectral types later than M6 (Briceño et al. 2002; Herbig 1998; Luhman 1999; Luhman et al. 2003). For their entire sample of low-mass stars and brown dwarfs, Liu et al. (2003) found a disk fraction of  $77 \pm 15\%$ , which is a factor of two larger than our measurements for IC 348. Among the 28 members of

IC 348 from the sample of Liu et al. (2003) for which [3.6]-[4.5] and [4.5]-[5.8] are available, only 11 objects show excesses in these colors. We find that 9/10 objects with  $E(K - L') > 0.2$  in the data from Liu et al. (2003) do indeed exhibit significant excesses in the IRAC colors. However, the putative detections of disks with smaller *L'* excesses from Liu et al. (2003) are not confirmed by the IRAC measurements. Because the color excess produced by a disk grows with increasing wavelengths, any bona fide detection of a disk at *L'* would be easily verified in the IRAC data.

Our IRAC images of IC 348 and Chamaeleon I have produced the most accurate, statistically significant measurements to date of disk fractions for brown dwarfs ( $> M6$ ). For both clusters, these measurements are consistent with the disk fractions exhibited by the stellar populations ( $M0-M6$ ,  $0.7 M_{\odot} \gtrsim M \gtrsim 0.1 M_{\odot}$ ). These results support the notion that stars and brown dwarfs share a common formation history, but do not completely exclude some scenarios in which brown dwarfs form through a distinct mechanism (Bate et al. 2003). The similarity of the disk fractions of stars and brown dwarfs also indicates that the building blocks of planets are available around brown dwarfs as often as around stars. The relative ease with which planets arise from these building blocks around stars and brown dwarfs remains unknown.

K. L. was supported by grant NAG5-11627 from the NASA Long-Term Space Astrophysics program.

<sup>7</sup> For objects in Chamaeleon I, we adopt the spectral types of Luhman (2004a).

## REFERENCES

- Apai, D., Pascucci, I., Sterzik, M. F., van der Blik, N., Bouwman, J., Dullemond, C. P., & Henning, Th. 2004, *A&A*, 426, L53  
 Baraffe, I., Chabrier, G., Allard, F., & Hauschildt, P. H. 1998, *A&A*, 337, 403  
 Bate, M. R., Bonnell, I. A., & Bromm, V. 2003, *MNRAS*, 339, 577  
 Briceño, C., Luhman, K. L., Hartmann, L., Stauffer, J. R., & Kirkpatrick, J. D. 2002, *ApJ*, 580, 317  
 Calvet, N., D'Alessio, P., Hartmann, L., Wilner, D., Walsh, A., & Sitko, M. 2002, *ApJ*, 568, 1008  
 Chabrier, G., Baraffe, I., Allard, F., & Hauschildt, P. H. 2000, *ApJ*, 542, 464  
 Comerón, F., Neuhäuser, R., & Kaas, A. A. 2000, *A&A*, 359, 269  
 Comerón, F., Reipurth, B., Henry, A., & Fernández, M. 2004, *A&A*, 417, 583  
 Fazio, G. G., et al. 2004, *ApJS*, 154, 10  
 Forrest, W. J., et al. 2004, *ApJS*, 154, 443  
 Haisch, K. E., Lada, E. A., & Lada, C. J. 2001, *ApJ*, 553, L153  
 Hartmann, L., et al. 2005, *ApJ*, 629, 881  
 Herbig, G. H. 1998, *ApJ*, 497, 736  
 Jayawardhana, R., Ardila, D. R., Stelzer, B., & Haisch, K. E. 2003, *AJ*, 126, 1515  
 Kenyon, S. J., & Hartmann, L. 1995, *ApJS*, 101, 117  
 Klein, R., Apai, D., Pascucci, I., Henning, Th., Waters, L. B. F. M. 2003, *ApJ*, 593, L57  
 Lada, C. J., Muench, A. A., Haisch, K. E., Lada, E. A., Alves, J. F., Tollestrup, E. V., & Willner, S. P. 2000, *AJ*, 120, 3162  
 Lada, C. J., Muench, A. A., Lada, E. A., & Alves, J. F. 2004, *AJ*, 128, 1254  
 Liu, M. C., Najita, J., & Tokunaga, A. T. 2003, *ApJ*, 585, 372  
 Luhman, K. L. 1999, *ApJ*, 525, 466  
 Luhman, K. L. 2004a, *ApJ*, 602, 816  
 Luhman, K. L. 2004b, *ApJ*, 614, 398  
 Luhman, K. L. 2004c, *ApJ*, 617, 1216  
 Luhman, K. L., et al. 2005a, *ApJ*, 620, L51  
 Luhman, K. L., Lada, E. A., Muench, A. A., & Elston, R. J. 2005b, *ApJ*, 618, 810  
 Luhman, K. L., Peterson, D. E., & Megeath, S. T. 2004, *ApJ*, 617, 565  
 Luhman, K. L., Rieke, G. H., Lada, C. J., & Lada, E. A. 1998, *ApJ*, 508, 347  
 Luhman, K. L., Stauffer, J. R., Muench, A. A., Rieke, G. H., Lada, E. A., Bouvier, J., & Lada, C. J. 2003, *ApJ*, 593, 1093  
 Luhman, K. L., & Steeghs, D. 2004, *ApJ*, 609, 917  
 Mohanty, S., Jayawardhana, R., Natta, A., Fujiyoshi, T., Tamura, M., & Barrado y Navascués, D. 2004, *ApJ*, 609, L33  
 Muench, A. A., Alves, J., Lada, C. J., & Lada, E. A. 2001, *ApJ*, 558, L51  
 Natta, A., & Testi, L. 2001, *A&A*, 376, L22  
 Pascucci, I., Apai, D., Henning, Th., & Dullemond, C. P. 2003, *ApJ*, 590, L111  
 Persi, P., et al. 2000, *A&A*, 357, 219  
 Reach, W. T., et al. 2005, *PASP*, 117, 978  
 Sterzik, M. F., Pascucci, I., Apai, D., van der Blik, N., & Dullemond, C. P. 2004, *A&A*, 427, 245

TABLE 1  
SUMMARY OF IRAC MAPS IN IC 348 AND CHAMAELEON I

| Target           | 3.6/5.8 Center     | 4.5/8.0 Center     | Dimensions<br>(arcmin) | Angle <sup>a</sup><br>(degrees) | Exp Time <sup>b</sup><br>(sec) | Date<br>(UT) |
|------------------|--------------------|--------------------|------------------------|---------------------------------|--------------------------------|--------------|
| IC 348           | 03 43 24 +32 07 03 | 03 44 18 +32 13 47 | 33 × 29                | 170                             | 20.8                           | 2004 Feb 11  |
| IC 348           | 03 44 44 +32 05 50 | 03 44 37 +32 12 27 | 15 × 15                | 79                              | 1548.8                         | 2004 Feb 18  |
| Cha I-N          | 11 09 26 -76 36 26 | 11 10 16 -76 30 20 | 33 × 29                | 28                              | 20.8                           | 2004 Jul 4   |
| Cha I-S          | 11 07 44 -77 34 46 | 11 07 48 -77 28 03 | 33 × 29                | 3                               | 20.8                           | 2004 Jun 10  |
| Cha I-S          | 11 08 46 -77 37 19 | 11 06 45 -77 39 37 | 20 × 15                | 72                              | 968                            | 2004 Feb 19  |
| Cha I-S          | 11 06 41 -77 39 09 | 11 08 47 -77 37 55 | 20 × 15                | 80                              | 968                            | 2004 Sep 2   |
| 2M J1101-7732A+B | 11 02 00 -77 35 17 | 11 00 43 -77 29 58 | 12 × 5                 | 144                             | 52                             | 2005 May 9   |

<sup>a</sup>Position angle of the long axis of the maps.

<sup>b</sup>Total exposure time for each position and filter.

TABLE 2  
IRAC PHOTOMETRY FOR LATE-TYPE MEMBERS OF IC 348

| ID                | Sp Type <sup>a</sup> | [3.6]      | [4.5]      | [5.8]      | [8.0]      |
|-------------------|----------------------|------------|------------|------------|------------|
| 291               | M7.25                | 11.94±0.02 | 11.57±0.02 | 11.14±0.04 | 10.39±0.07 |
| 316               | M6.5                 | 12.60±0.02 | 12.51±0.02 | 12.40±0.05 | 11.91±0.14 |
| 329               | M7.5                 | 12.87±0.02 | 12.77±0.02 | 12.72±0.06 | 12.67±0.25 |
| 355               | M8                   | 12.97±0.02 | 12.83±0.02 | 12.47±0.12 | ...        |
| 363               | M8                   | 13.19±0.02 | 13.11±0.02 | 13.02±0.03 | 13.02±0.13 |
| 405               | M8                   | 13.43±0.02 | 13.29±0.02 | ...        | ...        |
| 407               | M7                   | 14.03±0.02 | 13.70±0.04 | 13.16±0.04 | 12.39±0.08 |
| 415               | M6.5                 | 12.83±0.03 | 12.37±0.03 | 11.96±0.11 | ...        |
| 437               | M7.25                | 13.61±0.02 | 13.42±0.03 | 13.70±0.08 | ...        |
| 468               | M8.25                | 13.31±0.02 | 12.80±0.03 | 12.24±0.04 | 11.47±0.09 |
| 478               | M6.25                | 13.90±0.02 | 13.59±0.02 | 13.19±0.13 | ...        |
| 603               | M8.5                 | 14.18±0.05 | 13.94±0.07 | 13.73±0.08 | ...        |
| 611               | M8                   | 14.47±0.08 | 14.31±0.08 | ...        | ...        |
| 613               | M8.25                | 14.96±0.08 | 15.10±0.19 | ...        | ...        |
| 624               | M9                   | 15.94±0.19 | 15.69±0.21 | ...        | ...        |
| 690               | M8.75                | 14.65±0.04 | 14.23±0.05 | 13.93±0.12 | ...        |
| 703               | M8                   | 14.36±0.03 | 13.92±0.03 | 13.70±0.09 | ...        |
| 705               | M9                   | 15.13±0.06 | 14.86±0.05 | ...        | ...        |
| 738               | M8.75                | 15.24±0.04 | 14.89±0.03 | ...        | ...        |
| 761               | M7                   | 14.73±0.10 | 14.38±0.10 | ...        | ...        |
| 906               | M8.25                | 15.35±0.03 | 15.19±0.03 | ...        | ...        |
| 935               | M8.25                | 14.55±0.02 | 14.54±0.03 | ...        | ...        |
| 1050 <sup>b</sup> | >M8.5                | 15.07±0.07 | 14.91±0.04 | ...        | ...        |
| 2103 <sup>b</sup> | >M8.5                | 15.67±0.05 | 15.58±0.04 | ...        | ...        |
| 4044              | M9                   | 15.23±0.09 | 14.79±0.04 | ...        | ...        |

<sup>a</sup>From Luhman et al. (1998), Luhman (1999), Luhman et al. (2003), and Luhman et al. (2005b).

<sup>b</sup>Candidate members (Luhman et al. 2005b).

TABLE 3  
IRAC PHOTOMETRY FOR LATE-TYPE MEMBERS OF CHAMAELEON I

| ID                        | Sp Type <sup>a</sup> | [3.6]      | [4.5]      | [5.8]      | [8.0]      |
|---------------------------|----------------------|------------|------------|------------|------------|
| 2MASS 11011926-7732383A+B | M7.25+M8.25          | 11.00±0.01 | 10.86±0.01 | 10.83±0.01 | 10.76±0.02 |
| CHSM 17173                | M8                   | 11.96±0.01 | 11.87±0.01 | 11.71±0.03 | 11.76±0.04 |
| 2MASS 11085176-7632502    | M7.25                | 12.43±0.01 | 12.28±0.01 | 12.27±0.05 | 12.21±0.07 |
| OTS 44                    | M9.5                 | 13.71±0.02 | 13.21±0.02 | 12.76±0.04 | 12.04±0.02 |
| 2MASS 11084952-7638443    | M9                   | 13.61±0.01 | 13.21±0.02 | 12.68±0.06 | 12.14±0.04 |
| ISO 217                   | M6.25                | 10.79±0.01 | 10.29±0.01 | 9.85±0.01  | 9.17±0.03  |
| 2MASS 11100658-7642486    | M9.25                | 14.48±0.03 | 14.25±0.03 | ...        | 13.98±0.14 |
| 2MASS 11114533-7636505    | M8                   | 13.35±0.01 | 12.92±0.02 | 12.69±0.06 | 12.16±0.05 |
| 2MASS 11104006-7630547    | M7.25                | 12.83±0.01 | 12.71±0.01 | 12.59±0.05 | 12.63±0.06 |
| Cha H $\alpha$ 11         | M7.25                | 12.98±0.01 | 12.75±0.02 | 12.50±0.04 | 12.05±0.06 |
| 2MASS 11112249-7745427    | M8.25                | 13.55±0.01 | ...        | 12.80±0.04 | ...        |
| Cha H $\alpha$ 12         | M6.5                 | 11.34±0.01 | 11.27±0.03 | ...        | 11.13±0.03 |
| Cha H $\alpha$ 10         | M6.25                | 12.79±0.01 | 12.68±0.02 | 12.61±0.05 | 12.59±0.06 |
| ISO 138                   | M6.5                 | 12.50±0.02 | 12.21±0.01 | 11.97±0.03 | 11.30±0.02 |
| 2MASS 11082570-7716396    | M8                   | ...        | 13.01±0.01 | ...        | 11.95±0.03 |
| 2MASS 11093543-7731390    | M8.25                | 13.81±0.01 | 13.70±0.01 | 13.63±0.05 | 13.53±0.04 |
| Cha H $\alpha$ 1          | M7.75                | 11.56±0.01 | 11.15±0.02 | 10.76±0.01 | 9.67±0.02  |
| Cha H $\alpha$ 7          | M7.75                | 11.89±0.01 | 11.75±0.01 | 11.70±0.04 | 11.63±0.03 |

<sup>a</sup>From Luhman (2004a), Luhman (2004b), Luhman et al. (2004), and Luhman (in preparation).

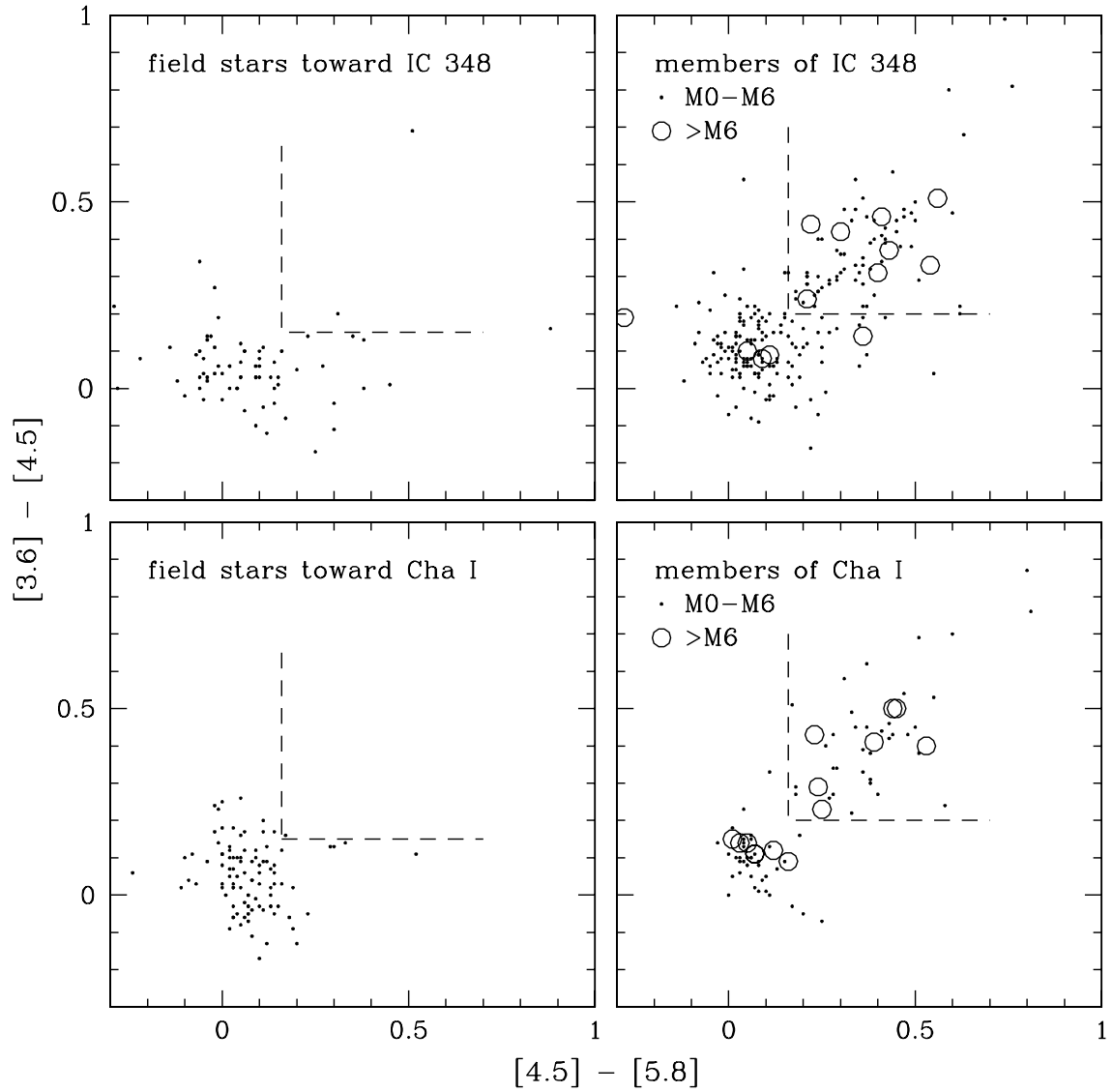


FIG. 1.— *Spitzer* IRAC color-color diagrams for the IC 348 and Chamaeleon I star-forming clusters. *Left*: Known field stars toward each cluster illustrate the spread in colors that arises from photometric errors. Relative to average colors of  $[3.6] - [4.5] = 0.05$  and  $[4.5] - [5.8] = 0.06$ , nearly all of the field stars have color excesses less than 0.1 in at least one color (*dashed line*). *Right*: Among the known members of each cluster, objects with disks are identified by excesses greater than 0.1 in both colors, which correspond to  $[3.6] - [4.5] \gtrsim 0.2$  and  $[4.5] - [5.8] \gtrsim 0.16$  for the M spectral types in these samples (*dashed line*).